In-situ measurement of the surface temperature during holographic recording

A. Draude[1], R. Meinhardt[1], H. Franke[1], Y. Zhao[2], and R. A. Lessard[3]

[1]*Department of Physics/Applied Physics, University of Duisburg-Essen, Lotharstr. 1, 47057 Duisburg, Germany*

[2]*Département de chimie, Université de Sherbrooke, Sherbrooke, Québec, Canada J1K 2R1*

[3]*COPL, Département de physique, génie physique et optique, Université Laval, Québec, Canada G1K7P4*

Received April 12, 2007

Photo-induced processes in organic materials mostly occur on molecular levels. Excited molecules may split to form radicals, starting a polymerization process with diffusing monomers. The azo-dyes perform an optically induced cis-trans isomerization. During pattern formation like a holographic grating, the local temperature increase, especially in thin films, is up to date a subject of estimation from absorption and dissipation data. However, the exact knowledge of the surface temperature would help a lot in understanding the resulting refractive index and thickness patterns during holographic exposure. In this paper, *in-situ* pyrometer measurements are presented. As examples, different photosensitive materials, varying from a photopolymer to polycrystalline azo dyes, are used in order to outline the magnitude of this effect and demonstrate the feasibility of this technique.

OCIS codes: 050.1940, 090.2900, 160.2900, 350.5340.

Recording a light pattern in a photosensitive material generally means a series of processes in the material system. The absorption of the initiating photons is usually the first activating step[1]. After the photon energy is absorbed, the excitation may be followed by a molecular transition, an initiation of polymerization[2,3], etc.. Any local chemical process leads to diffusion and in some cases even material transport[4−7]. In the presence of oxygen, a photo-induced oxidation may occur[8]. Endothermic and exothermic reactions may be involved. Some reactions mainly occur at elevated temperatures. In the case of self developing photo etching, e.g. with excimer laser radiation, material decomposition may occur[9].

In all these different cases, an interesting question is what the temperature is during recording. Therefore we present a straight forward experimental technique using a pyrometer for measuring the temperature during the holographic exposure. We do this investigation for different material systems, a volume photopolymer[2,3,10−13] and thin films with active azobenzene groups in different concentrations like guest-host systems[14−17], side-chain polymers[4,5,18−22], or organic glasses[23−26].

Measurements have been carried out as a scan through the cross section of the exposed area and for a center spot as a function of recording time. A temperature increase of up to 25 K has been found depending on the material. The time-dependent measurements indicate different processes like refractive index pattern formation or material transport.

The experimental arrangement used in this investigation is shown in Fig. 1 with a schematic and a photo of the measuring part. The conventional two-beam holographic recording set-up with an Ar-ion laser at the wavelength $\lambda = 488$ nm is completed by a pyrometer (see Fig. 1, Voltcraft IR-1001A), which is mounted on an x-stage parallel to the grating vector in the sample in a distance of 16.7 cm. The pyrometer numerical reading is recorded by a digital camera and then correlated to the particular x-position. The measured spot size of the pyrometer in this geometry is about 3.3 mm in diameter (50:1 optic of pyrometer) which is well below the exposed spot size of 6-mm diameter. Therefore an "x-scan" for the temperature measurement can be performed during holographic exposure.

The measurements work as follows. The temperature-dependent radiation power of a black body emitting into the solid angle $\Omega = 2\pi$ (half space), measured by the pyrometer's infrared (IR)-detector can be written as[27]

$$P_{\mathrm{bB}}(T) = k \int_{\Delta f} w_{\mathrm{bB}}(f)\mathrm{d}f \qquad (1)$$

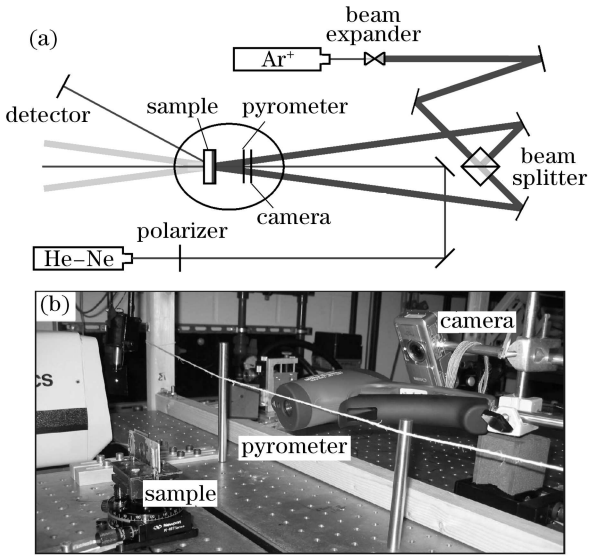

Fig. 1. Experimental arrangement for the *in-situ* measurement of the surface temperature during holographic recording. (a) Schematic; (b) photograph of the measuring part.

with $w_{\mathrm{bB}}(f)\mathrm{d}f$ being the emitted energy density given by Planck's radiation law[27],

$$w_{\mathrm{bB}}(f)\mathrm{d}f = \frac{8\pi h f^3}{c^3}\frac{\mathrm{d}f}{1-\exp[hf/(kt)]}, \quad (2)$$

where c is the speed of light, h is the Planck's constant, k is the Boltzmann constant, f is frequency, the constant $k = A\Omega c/(4\pi)$ is determined by the pyrometer's specifications, A is the area of detector, Ω is the solid angle of measurable radiation given by the pyrometer's optics (IR-1001A, distance to spot ratio $50:1 \rightarrow \Omega = \pi(1/2)^2/50^2 = \pi \times 10^{-4}$ rad for plane surfaces).

For general non-black bodies, the emitted energy density is proportional to that of the black body[27]:

$$w_{\mathrm{gB}}(f)\mathrm{d}f = \varepsilon(f) w_{\mathrm{bB}}(f)\mathrm{d}f, \quad (3)$$

where $\varepsilon(f)$ is the frequency-dependent emissivity of the body. If the frequency interval Δf is small enough, the emissivity becomes constant and the measured radiation power can be written as

$$P_{\mathrm{gB}}(T) = \varepsilon P_{\mathrm{bB}}(T). \quad (4)$$

For organic materials, the value of the emissivity is $\varepsilon = 0.95$[28,29]. This value can be verified by comparing the temperature of the sample's surface at laboratory conditions measured by the pyrometer with the temperature measured by an independent thermometer (like commercial mercury thermometer).

The experimental set-up shown in Fig. 1 allows the *in-situ* measurement of the diffraction efficiencies using a He-Ne laser ($\lambda = 633$ nm) as well.

In Fig. 2, a typical x-scan curve for the pyrometer is presented for a holographic experiment with the azo-dye disperse red I (DR1). The sample was prepared by evaporating DR1 molecules from the vapor phase in an average thickness of 600 nm (reading from the thickness monitor, DEKTAK profilometer scan)[30,31]. Depending on the substrate's surface charge or the substrate's polarity, two different types of layers can be produced, either a transparent layer of preoriented molecules or a highly scattering layer[30,31]. For such a system, a thin grating with a diffraction efficiency for the first order of a few percentage is obtained[26] (Fig. 3(a)). Atomic force microscopy (AFM) investigations indicate a clear surface grating. The material processes involved here are cis-trans photoisomerization[32–34], material transport (relief grating)

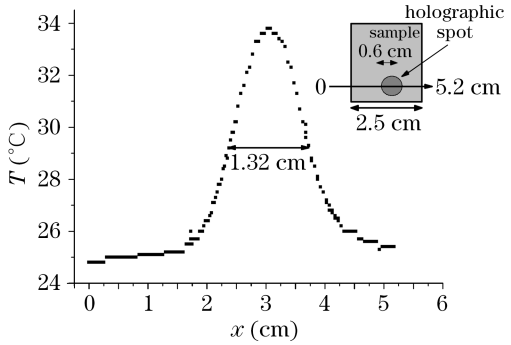

Fig. 2. Temperature measurement with x-scan during holographic recording in 600-nm thick DR1 on glass, dimensions are shown in the inset.

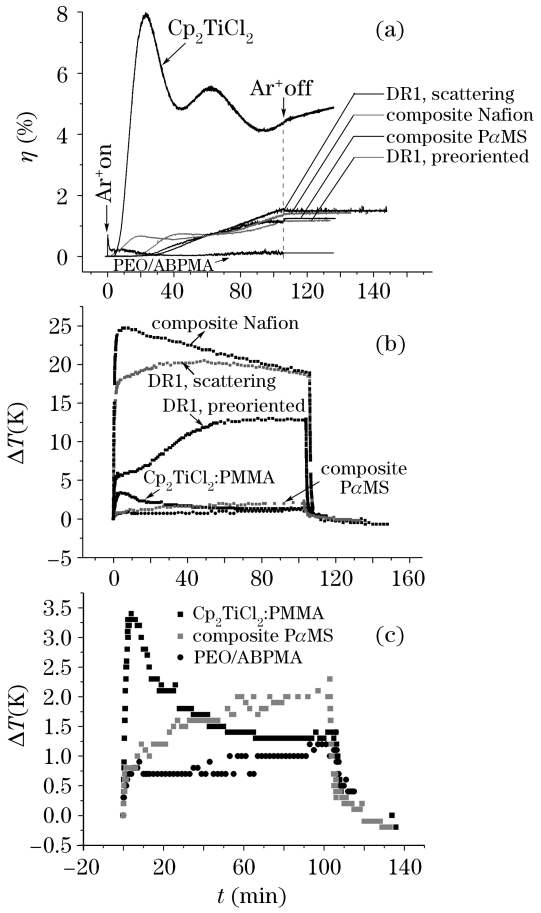

Fig. 3. (a) Diffraction efficiency η for the first order diffraction as a function of recording time for different holographic materials (see Table 1); (b) temperature measurements for the corresponding material systems of (a); (c) lower curves with higher resolution in (b).

and crystallization and melting phenomena. The x-scan was performed with a stepping motor.

However the local variation of the surface temperature is quite evident with a maximum change of $\Delta T_{\max} = 9$ K in this example ($34 - 25$ °C). The DR1 system shown in Fig. 2 is among those we investigate in this paper with an average recording temperature (Fig. 3(b), DR1, preoriented, maximum temperature difference $\Delta T = 12.9$ K). The temperature π-scan measurement has been performed $\sim$ 30 min after the start of recording, which explains the low value of $\Delta T_{\max}$ in Fig. 3(b). The Gaussian profile of the holographic interference pattern is reflected in the temperature profile. Caused by heat transmission, the full-width at half-maximum (FWHM) value of 1.32 cm highly exceeds the diameter of the holographic spot of 0.6 cm.

Similar measurements have been performed with some other quite different organic photo-sensitive systems (see Table 1). In order to compare different materials, we measured the diffraction efficiency η and the maximum temperature T during and after the recording process. Both quantities were measured in the center of the exposed spot, which refers to the maximum in the temperature curve in Fig. 2. The grating constant was chosen to be $\Lambda = 2$ μm, the recording time $t_{\mathrm{rec}} = 106$ min, and the recording intensity per beam $I = 4880$ W/m^2 ($\lambda = 488$ nm) in all measurement results, as shown in Fig. 3.

Table 1. Material Systems for Monitoring the Temperature during Holographic Recording

Label	Material System
DR1, Scattering	Substrate/600-nm DR1 (Red, Highly Scattering)
DR1, Preoriented	Substrate/600-nm DR1 (Transparent, Preoriented)
Cp_2TiCl_2:PMMA	Substrate/4.3-mm PMMA:Cp_2TiCl_2 (Photopolymer)
Composite PαMS	1.8-μm Poly(alpha-methylstyrene) (PαMS)/600-nm DR1 (Transparent)
PEO/ABPMA	1.08-μm PEO/ABPMA (Side-Chain Polymer)
Composite Nafion	Substrate/245-nm Nafion/600-nm DR1 (Red)

Substrate: microscope slides, Menzel, dimensions $7.5 \times 2.5 \times 0.1$ (cm), refractive index $n = 1.521$.

Regarding $\eta(t)$, the material systems can be divided into three different classes. The photopolymer poly(methyl methacrylate): titanocendichloride (PMMA:Cp_2TiCl_2) shows the highest value of the diffraction efficiency up to $\sim 8\%$ (Fig. 3(a)). For this thick-grating system[35], η-values up to 100% are measured depending on the reading angle's difference to the Bragg-angle[3]. After stopping the holographic exposure, the sample develops, and this process can be rapidly accelerated using heat[3]. The second class contains all systems with concentrated DR1 as the upper layer. These thin-grating systems show η-values between 1.15% and 1.5% after the recording time $t_{\rm rec} = 106$ min. After switching off the Ar^+ light, the diffraction efficiency remains constant. The side-chain polymer PEO/ABPMA represents the third class (also thin grating). It shows a maximum in $\eta(t)$ after a few seconds of recording. In a second experiment, a clear surface-relief grating could be detected at this point (AFM). With increasing recording time, the diffraction efficiency and the surface grating decay. After the holographic exposure, η remains constant. While for the first two system classes, the diffraction efficiency still develops at the time of the Ar^+ light's turning off, and the side-chain polymer saturates at $t \sim 40$ min.

Figures 3(b) and (c) show the $T(t)$ behavior. All curves show a rapid increase in the temperature at the beginning of the holographic exposure and a fast decrease to laboratory temperature after the laser beams are switched off. The latter behavior can be assumed as an exponential decay with a decay time of $t_{\rm dec} \sim 30$ s (for all samples!). Heat is transferred to the environment and transformed into heat radiation; these processes are typical for all samples. At the beginning of the holographic exposure, a part of the energy of the holographic radiation is transformed into heat. The height of the peak is related with exemption of the photopolymer to the absorbance ($= -\lg(I/I_0)$) of the samples, a high value at $\lambda = 488$ nm results in a high peak (Table 2).

Table 2. Absorbance of the Samples Measured with a Spectrometer at λ=488 nm

Sample	Absorbance $-\lg(I/I_0)$
DR1, Scattering	1.8027
DR1, Preoriented	0.265
Cp_2TiCl_2:PMMA	0.0672
Composite PαMS	0.1523
PEO/ABPMA	0.1853
Composite Nafion	2.1232

The shape of the $T(t)$ curves may be affected by the heat conduction σ of the different substrates. If σ is high, heat can be transferred away from the substrate easily and the surface remains relatively cool. This is shown by the comparison between the systems of PαMS and preoriented DR1 (see Table 1, Fig. 3). Both systems show a similar behavior of $\eta(t)$ and absorbance, but the $T(t)$ curves are much different. PαMS seems to have a high value of σ, therefore heat is easily transferred to the glass substrate and the surface remains relatively cool ($\Delta T_{\rm max} \leq 2.25$ K). In case of glass, much more heat stays at the surface ($\Delta T_{\rm max} \leq 12.9$ K). During the recording process, Nafion seems to change its heat conducting properties. At the beginning of the experiment, σ seems to be higher than that of glass, while with increasing time both values approach to each other (comparing systems DR1 scattering/composite Nafion, see Fig. 3(b)). In the case of PEO/ABPMA, the absorption coefficient is low, most of the light transmits through the sample and the surface temperature remains low. Polymeric reactions can be monitored regarding the photopolymer system. The temperature maximum at the beginning refers to the exothermic split reaction of the photo initiator Cp_2TiCl_2 ($\Delta T_{\rm max} = 3.5$ K, Fig. 3(c)). After this process, the radicalic polymerization of the residual monomers, which are still inside the polymer matrix, follows. The temperature decreases because the speed of the latter reactions decreases due to monomer exhaustion and the absorbance decreases due to photo-starter exhaustion.

The actual temperature of the sample surface may be regarded as a measure for chemical reactions or physical changes of involved phases like melting or growing of crystalline domains with subsequent surface relief formation or reorientation of domains. Therefore the $T(t)$ dependence may be used in correlation with the corresponding $\eta(t)$ curve for the interpretation of the specific processes occurring in a photosensitive system.

Finally it should be mentioned that clean glass substrates do not show a temperature change during holographic exposure.

In conclusion, the online recording of the surface temperature of photosensitive samples during holographic recording is possible with sufficient local resolution. *In-situ* measurements across the sample ($T(x)$ scans) or measurements as a function of time for the maximum value $T(t)$ are presented for different exemplary material systems. The $T(t)$ curves in combination with the diffraction efficiencies $\eta(t)$ reveal more information about materials. The highest recording tempera-

tures were found in the beginning of the recording. Interestingly enough this corresponds to maxima in the diffraction efficiencies of recorded gratings in most azo compounds. After this early recording period of high efficiencies and high local temperature, the material systems seem to relax into a period of equilibrium, passing thermal energy to the environment. The reported *in-situ* measurement of the surface temperature during holographic recording also gives an estimate of reaction temperatures during recording. This helps understanding local chemical or physical changes, especially in thin films ($\leq$ 1 μm). In special systems, for instance, the glass transition temperature may be reached during optical recording. For the resolution of multi-step material processing, more detailed investigations are necessary with specific materials.

A. Draude's e-mail address is ansgar.draude@uni-due.de.

References

1. L. Solymar and D. J. Cooke, *Volume Holography and Volume Gratings* (Academic Press, New York, 1981).
2. M. Kopietz, M. D. Lechner, D. G. Steinmeier, J. Marotz, H. Franke, and E. Krätzig, Polymer Photochem. **5,** 109 (1984).
3. A. Draude, H. Franke, and R.A. Lessard, J. Phys. D **38,** 974 (2005).
4. P. Rochon, E. Batalla, and A. Natansohn, Appl. Phys. Lett. **66,** 136 (1995).
5. D. Y. Kim, S. K. Tripathy, L. Li, and J. Kumar, Appl. Phys. Lett. **66,** 1166 (1995).
6. P. Lefin, C. Fiorini, and J.-M. Nunzi, Pure Appl. Opt. **7,** 71 (1998).
7. A. D. Rey and M. M. Denn, Annu. Rev. Fluid Mech. **34,** 233 (2002).
8. A. Peled, (ed.) *Photo-Excited Processes, Diagnostics and Applications: Fundamentals and Advanced Topics* (Kluwer, Boston, 2003).
9. I. W. Boyd, *Laser Processing of Thin Films and Microstructures: Oxidation, Deposition, and Etching of Insulators* (Springer, Berlin, 1988).
10. R. A. Lessard and G. Manivannan, (eds.) *Selected Papers on Photopolymers, vol. 114 of SPIE Milestone Series* (SPIE, Bellingham, 1996).
11. K. Pacheco, G. Aldea, C. Cassagne, and J.-M. Nunzi, Proc. SPIE **6343,** 634330 (2006).
12. Y. Tomita, Y. Endoh, N. Suzuki, and K. Furushima, Proc. SPIE **6343,** 634331 (2006).
13. R. Birabassov, O. Pouraghajani, S. Peredereeva, S. Deblois, J. Tourigny, N. Ashurbekov, and R. A. Lessard, Proc. SPIE **6343,** 634333 (2006).
14. K. Prasuhn, A. Draude, H. Franke, and R. A. Lessard, Proc. SPIE **5578,** 658 (2004).
15. A. Y.-G. Fuh, C.-R. Lee, and Y.-H. Ho, Appl. Opt. **41,** 4585 (2002).
16. A. Y.-G. Fuh, C.-R. Lee, and K.-T. Cheng, Jpn. J. Appl. Phys. **42,** 4406 (2003).
17. M. Ivanov, T. Todorov, L. Nikolova, N. Tomova, and V. Dragostinova, Appl. Phys. Lett. **66,** 2174 (1995).
18. J. Yang, J. Zhang, J. Liu, P. Wang, H. Ma, H. Ming, Z. Li, and Q. Zhang, Opt. Mater. **27,** 527 (2004).
19. D. Y. Kim, L. Li, X. L. Jiang, V. Shivshankar, J. Kumar, and S. K. Tripathy, Macromolecules **28,** 8835 (1995).
20. I. Mancheva, I. Zhivkov, and S. Nešpurek, J. Optoelectron. and Adv. Mater. **7,** 253 (2005).
21. M. Bolte, Y. Israëli, A. Rivaton, and R. A. Lessard, Proc. SPIE **6343,** 63432U (2006).
22. L. Nikolova, T. Todorov, M. Ivanov, F. Andruzzi, S.Hvilsted, and P. S. Ramanujam, Appl. Opt. **35,** 3835 (1996).
23. T. Fuhrmann and T. Tsutsui, Chem. Mater. **11,** 2226 (1999).
24. A. Draude, N. Reinke, A. Perschke, H. Franke, R. A. Lessard, and T. Fuhrmann, Proc. SPIE **4833,** 602 (2002).
25. N. Reinke, A. Draude, T. Fuhrmann, H. Franke, and R. A. Lessard, Appl. Phys. B **78,** 205 (2004).
26. R. Meinhardt, A. Draude, H. Franke, and R. A. Lessard, Proc. SPIE **6343,** 634336 (2006).
27. E. Hecht, *Physics* (Wadsworth, Belmont, 1994).
28. Voltcraft, *Infrared-Thermometer IR-1001A, Operating Instructions* (in German) (Voltcraft, Hirschau, 2004).
29. IMPAC Infrared GmbH, *Pyrometerhandbuch* (in German) (IMPAC Infrared GmbH, Frankfurt, 2004).
30. S. Verpoort, A. Draude, R. Meinhardt, H. Franke, and R. A. Lessard, J. Appl. Phys. **100,** 023504 (2006).
31. S. Verpoort, A. Draude, H. Franke, and R. A. Lessard, Proc. SPIE **6343,** 634334 (2006).
32. A. Teitel, Naturwissenschaften (in German) **44,** 370 (1957).
33. T. Todorov, L. Nikolova, and N. Tomova, Appl. Opt. **23,** 4309 (1984).
34. T. Fuhrmann, "Azo- und stilbenhaltige Seitenkettenpolymere für optische Datenspeicher und Holographsiche Optische Elemente", Dissertation (in German) (University of Marburg, 1997).
35. W. R. Klein and B. D. Cook, IEEE Trans. Son. Ultrason. **14,** 123 (1967).